Published September 17, 2012

A PHD12–Snail2 repressive complex epigenetically mediates neural crest epithelial-to-mesenchymal transition

Pablo H. Strobl-Mazzulla[1] and Marianne E. Bronner[2]

[1]Biología del Desarrollo, Instituto de Investigaciones Biotecnológicas–Instituto Tecnológico de Chascomús, Consejo Nacional de Investigaciones Científicas y Técnicas–Universidad Nacional de San Martín, 7130 Chascomús, Argentina
[2]Division of Biology 139-74, California Institute of Technology, Pasadena, CA 91125

Neural crest cells form within the neural tube and then undergo an epithelial to mesenchymal transition (EMT) to initiate migration to distant locations. The transcriptional repressor Snail2 has been implicated in neural crest EMT via an as of yet unknown mechanism. We report that the adaptor protein PHD12 is highly expressed before neural crest EMT. At cranial levels, loss of PHD12 phenocopies Snail2 knockdown, preventing transcriptional shutdown of the adhesion molecule Cad6b (Cadherin6b), thereby inhibiting neural crest emigration. Although not directly binding to each other, PHD12 and Snail2 both directly interact with Sin3A in vivo, which in turn complexes with histone deacetylase (HDAC). Chromatin immunoprecipitation revealed that PHD12 is recruited to the Cad6b promoter during neural crest EMT. Consistent with this, lysines on histone 3 at the Cad6b promoter are hyperacetylated before neural crest emigration, correlating with active transcription, but deacetylated during EMT, reflecting the repressive state. Knockdown of either PHD12 or Snail2 prevents Cad6b promoter deacetylation. Collectively, the results show that PHD12 interacts directly with Sin3A/HDAC, which in turn interacts with Snail2, forming a complex at the Cad6b promoter and thus revealing the nature of the in vivo Snail repressive complex that regulates neural crest EMT.

Introduction

The epithelial to mesenchymal transition (EMT) is a process, important in embryogenesis and cancer, by which epithelial cells are converted from a tightly adherent sheet of cells into a more dispersed mesenchymal population. One embryonic cell type that undergoes EMT is the neural crest. This transient population arises during neurulation within the neuroepithelium. Upon neural tube closure, these cells emigrate from the dorsal neural tube via EMT and subsequently migrate extensively to contribute to numerous derivatives (Le Douarin and Kalcheim, 1999).

Some of the molecular players involved in aspects of EMT have been characterized. For example, transcriptional regulators like Snail, Sip1, and FoxD3 directly regulate downstream targets to trigger intracellular responses and guide major cytoskeletal rearrangements as well as changes in cell junctions and adhesion properties (Thiery and Sleeman, 2006; Sauka-Spengler and Bronner-Fraser, 2008; Strobl-Mazzulla and Bronner, 2012). In many systems, Snail transcription factors have been shown to repress regulatory regions of cadherins. For example, Snail inhibits E-cadherin expression in numerous cancer cells (Batlle et al., 2000; Cano et al., 2000; Bolós et al., 2003), and Snail2 directly represses Cad6b (Cadherin6b) in premigratory neural crest cells (Hatta et al., 1987; Nakagawa and Takeichi, 1995; Taneyhill et al., 2007). Despite the fact that Snail-mediated repression is well documented in numerous EMTs (Hemavathy et al., 2000; Nieto, 2002; Barrallo-Gimeno and Nieto, 2005; Pérez-Mancera et al., 2005), the molecular basis of this repression is largely unknown.

Correspondence to Marianne E. Bronner: mbronner@caltech.edu

Abbreviations used in this paper: BiFC, bimolecular fluorescence complementation; ChIP, chromatin IP; EMT, epithelial to mesenchymal transition; HDAC, histone deacetylase; IP, immunoprecipitation; ISH, in situ hybridization; MO, morpholino oligonucleotide; PHD, plant homeodomain; QPCR, quantitative PCR; spMO, splicing MO; ss, somite stage; tMO, translation MO; TSS, transcription start site.

Supplemental Material can be found at:
http://jcb.rupress.org/content/suppl/2012/09/13/jcb.201203098.DC1.html

The Rockefeller University Press $30.00
J. Cell Biol. Vol. 198 No. 6 999–1010
www.jcb.org/cgi/doi/10.1083/jcb.201203098

Published September 17, 2012

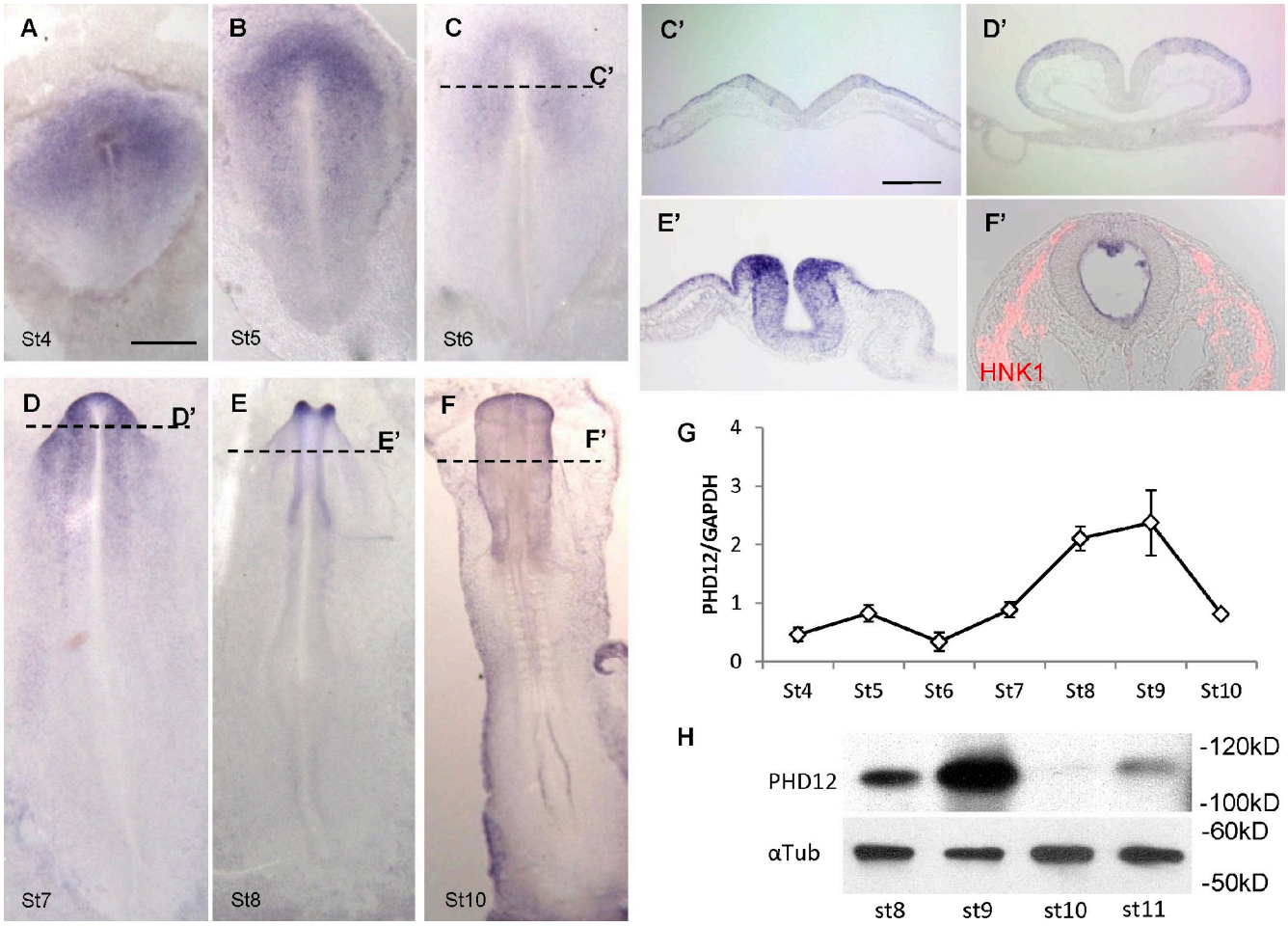

Figure 1. **PHD12 is expressed at times and locations correlating with neural crest EMT.** (A–F′) Expression pattern of PHD12 in the early chick embryo by whole-mount ISH at stages (St) 4–10. Transverse sections (dotted lines) reveal specific expression in the nonneural ectoderm and dorsal neural tube at stages 6–8 (C′–E′) and at low levels in migratory neural crest cells (identified by HNK-1 staining in red) at stage 10 (F′). (G) QPCR analyses show increasing PHD12 expression, peaking at stage 9 and decreasing thereafter at stage 10. Values represent the mean of three samples run in triplicate ± SD. (H) Western blot using PHD12 antibody on five pooled embryos at each stage. αTub, α-tubulin; GAPDH, glyceraldehyde 3-phosphate dehydrogenase. Bars: (A–F) 200 µm; (C′–F′) 100 µm.

One intriguing possibility is that Snail mediates the repression of cadherins by recruiting corepressors, which have yet to be identified. In the case of E-cadherin, it has been proposed by Peinado et al. (2004) that this corepressor complex contains histone deacetylase (HDAC) and Sin3A. Recruitment of HDAC would result in hypoacetylation of histone H3, which is a prerequisite for transcriptional repression. However, it is unknown whether or how Snail recruits these putative partners and/or whether this is a general mechanism involved in EMT.

In this study, we probe the molecular mechanisms underlying cranial neural crest EMT. In a screen for new transcriptional regulators functioning during neural crest development (Adams et al., 2008), we identified the chick homologue of human PHD12 (also known as Pf1) and here confirm its expression in newly induced neural crest cells. In cultured HEK293 cells, Pf1 has been shown to interact directly with mSin3A/HDAC (Yochum and Ayer, 2001). Analogously, we find in the in vivo context that PHD12 interacts directly with Sin3A, which in turn interacts with Snail2, resulting in recruitment of the HDAC complex to the promoter region of Cad6b. These results reveal for the first time the dual specificity of epigenetic regulators, such as PHD12, and transcription factors, such as Snail2, that act cooperatively to fine tune the process of neural crest EMT.

Results

PHD12 is highly expressed before neural crest EMT

PHD12 is expressed in a spatiotemporal pattern consistent with an important role in neural crest development (Fig. 1). PHD12 transcripts are present in the neural plate, neural plate border, and nonneural ectoderm during gastrulation by stage 4/5 (Fig. 1, A and B). As neurulation proceeds, PHD12 becomes restricted to the dorsal neural folds and nonneural ectoderm by stage 6–8 (Fig. 1, C–E). After neural tube closure, at stage 10, PHD12 expression is no longer observed on migrating HNK1+ cranial neural crest cells but still is present on the open neural folds at trunk levels (Fig. 1 F). Analysis by quantitative PCR (QPCR) and Western blotting confirmed that the

Published September 17, 2012

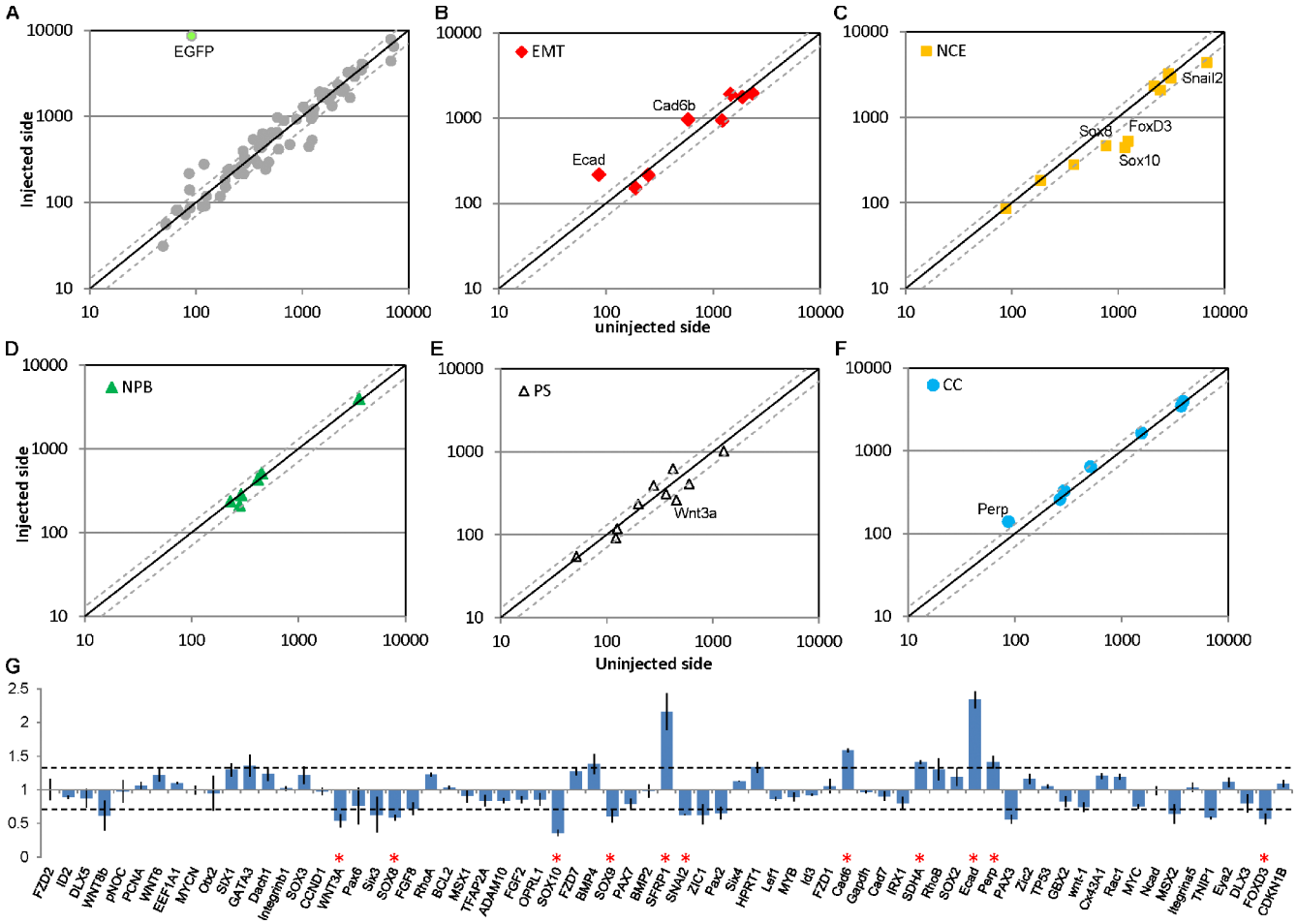

Figure 2. **NanoString analysis reveals that PHD12 loss of function affects Cad6b and neural crest specifier genes.** (A) Log scale scatter plot showing changes in expression of 70 genes in the dorsal neural tube on the PHD12-MO–injected versus uninjected side of a single representative embryo fixed at stage 9–10ss. (B–E) The analyzed genes were subdivided into categories corresponding to EMT genes (B); neural crest specifier (NCS) genes (C); neural plate border (NPB) genes (D); and patterning signal (PS) genes (E). Dotted lines represent 30% variation. Of the EMT genes, only E-cadherin (Ecad) and Cad6b were increased >30% on the PHD12-MO–injected side compared with the uninjected side of the same embryo. In contrast, the neural crest specifier genes Sox10, Snail2, FoxD3, and Sox9 were reduced on the morpholino-injected side. CC, cell cycle regulator. (G) Bar graph shows the mean of four embryos representing fold expression differences (means ± SD) between injected and uninjected side on PHD12-MO–treated embryos. Dotted lines in all graphs represent variation >30% between sides. Asterisks indicate significant differences ($P < 0.05$) on the injected side compared with the uninjected side analyzed by Student's *t* test. Gapdh, glyceraldehyde 3-phosphate dehydrogenase.

highest expression of PHD12 is at stage 8/9, correlating with the onset of neural crest EMT. Expression decreases dramatically after onset of neural crest migration (Fig. 1 G).

Loss of PHD12 leads to changes in Cad6b and neural crest genes during stages of emigration

To examine the function of PHD12, we tested the developmental effects of its loss of function on gene expression of newly formed cranial neural crest cells. To this end, we designed two distinct fluorescein-tagged morpholino oligonucleotides (MOs): one overlapping the ATG codon to block protein translation (plant homeodomain [PHD]-translation MO [tMO]) and the second to the second exon–intron boundary, preventing splicing (PHD-splicing MO [spMO]). MOs plus carrier DNA were injected on the left half of stage 4–5 embryos, such that the uninjected side served as an internal control. Although both morpholinos gave comparable results, the translation blocking morpholino was used in most cases. After electroporation, embryos were dissected in half and immunoblotted with a PHD12 antibody. The results show that the morpholinos caused a marked reduction of PHD12 protein on the injected side compared with the uninjected side of the same embryo or when compared with the injected side of control-MO (Ctrl-MO)–treated embryos (Fig. S1 A). RT-PCR analysis of PHD-spMO–treated embryos, using a set of primers located over the first and fourth exons, revealed the expected 417-bp band, also detected in Ctrl-MO–treated embryos, plus a 235-bp band (Fig. S1 B). Sequence analysis showed that the 235-bp band corresponds to an amplification product as a result of forced splicing between the first and third exons, excising the first two introns and the second exon. This generated a premature stop codon and a truncated protein lacking the two PHD zinc finger domains.

Although PHD12 morpholino was introduced during gastrulation, the first apparent phenotype was observed during initiation of neural crest migration. To assess the effects of PHD12 depletion on a large scale, we used nCounter technology (NanoString;

Published September 17, 2012

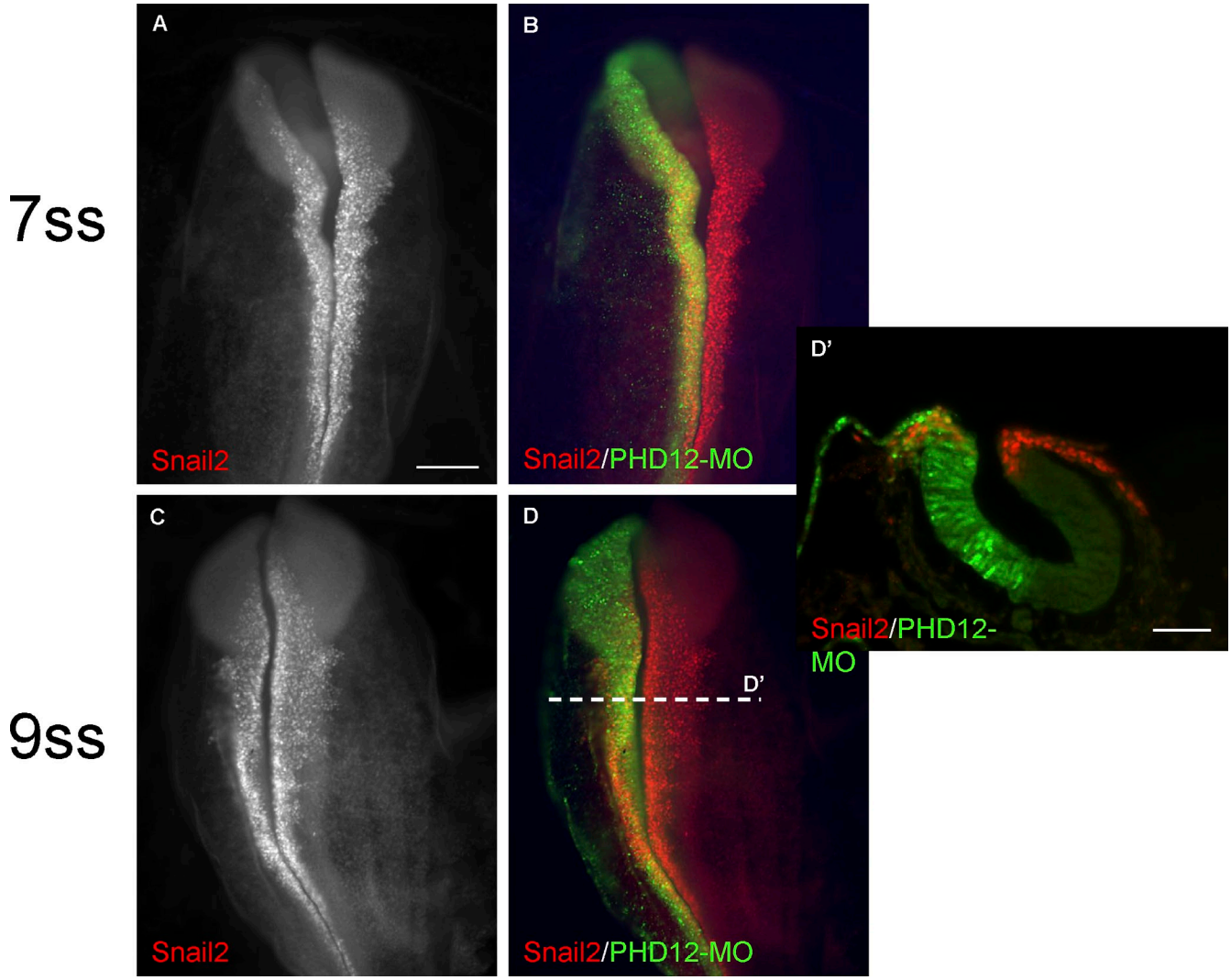

Figure 3. **PHD12 knockdown prevents neural crest emigration.** (A and B) Electroporation of fluorescent PHD12-MO into the left side of the embryo has no effect on Snail2 immunoreactive premigratory neural crest cells at the 7ss. (C and D) However, at 9ss, the Snail2+ neural crest cells appear unable to migrate on the morpholino-treated compared with the right uninjected side. (D′) Transverse section at the level of dotted line in D. Bars: (A–D) 100 µm; (D′) 50 µm.

Fortina and Surrey, 2008) to perform a multiplex analysis of changes in the transcript levels of 70 genes (Fig. 2) at the time of active neural crest emigration from the neural tube (9–10 somite stage [ss]). This included transcripts expressed in the neural crest, neural plate, neural plate border, neural tube, ectodermal placodes, and nonneural ectoderm as well as genes involved in proliferation and apoptosis. For NanoString analysis, dorsal neural tubes were dissected from each side of electroporated embryos, and each half was individually analyzed and compared. No significant differences were observed between the two sides of Ctrl-MO–treated embryos (unpublished data), with a <20% variation. As a consequence, we defined 30% (Fig. 2, dotted lines) variation as our cutoff for statistical significance. NanoString reads from individual dorsal neural tubes were plotted by comparing injected versus uninjected sides (Fig. 2 A) and then divided into groups of genes that correlate with the EMT (Fig. 2 B), neural crest specification (Fig. 2 C), neural plate border (Fig. 2 D) specification, patterning signals (Fig. 2 E), and cell cycle regulators (Fig. 2 F).

Of the EMT genes, only Cad6b and E-cadherin were up-regulated 1.6- and 2-fold, respectively. In contrast, neural crest specifier genes Sox8 (0.6-fold), Sox10 (0.4-fold), Snail2 (0.7-fold), and FoxD3 (0.6-fold) were down-regulated at the 9–10ss after PHD12 knockdown. No changes were observed in several neural plate border or cell cycle genes, with the exception of the *PERP* (*p53 apoptosis effector related to PMP-22*) gene, which was slightly up-regulated on the injected side. Of the patterning signals, only Wnt3a (0.5-fold) and SFRP1 (secreted frizzled-related protein 1) were altered on the injected side.

Loss of PHD12 does not alter neural crest specification but affects EMT

There are several possible explanations for the alterations in neural crest specifier and EMT-related genes after loss of PHD12. One possibility is that PHD12 may be required for the correct specification of the neural crest. Alternatively, an intriguing possibility is that there may be a failure in EMT.

Published September 17, 2012

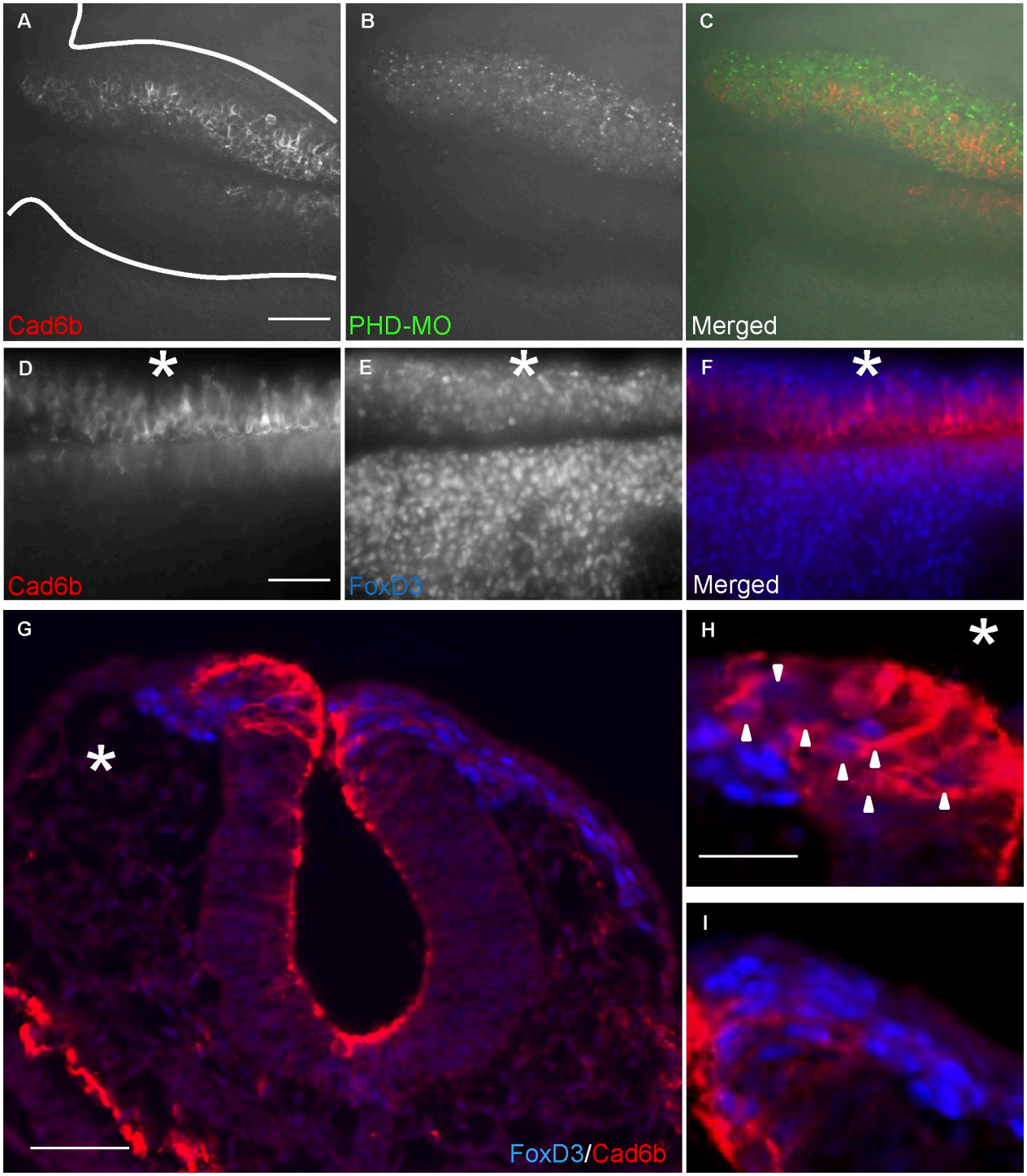

Figure 4. **PHD12 knockdown prevents Cad6b down-regulation and neural crest emigration.** (A–C) Confocal images of embryos treated with PHD12-MO reveal that Cad6b persists in the dorsal neural tube, at the midbrain level, and on the morpholino-treated side compared with the uninjected side. (D–F) Double immunohistochemistry shows that Cad6b expression is maintained, resulting in a paucity of migrating neural crest cells expressing FoxD3 on the PHD12-MO electroporated side (asterisks). (G–I) Transverse sections (G) and high magnification views of the dorsal neural tube (H and I) show colocalization of FoxD3- and Cad6b-expressing cells that appear unable to migrate on the injected side (arrowheads). Bars: (A–G) 50 µm; (H and I) 25 µm.

To distinguish between these possibilities and gain spatial information, we examined the expression patterns of neural crest specifier genes FoxD3 and Snail2 at the 5–6ss and 7ss, corresponding to the time when these neural crest markers are first observed on premigratory neural crest cells in the dorsal neural tube. At these early stages, no alterations were observed in these markers, suggesting that neural crest specification was unaffected (Fig. S2 and Fig. 3). However, by the 9ss, Snail2-positive neural crest cells appeared unable to migrate (Fig. 3) on the PHD12-MO–treated side of the embryos.

To confirm that we were affecting the EMT process, we examined the expression of Cad6b on morpholino-treated

Published September 17, 2012

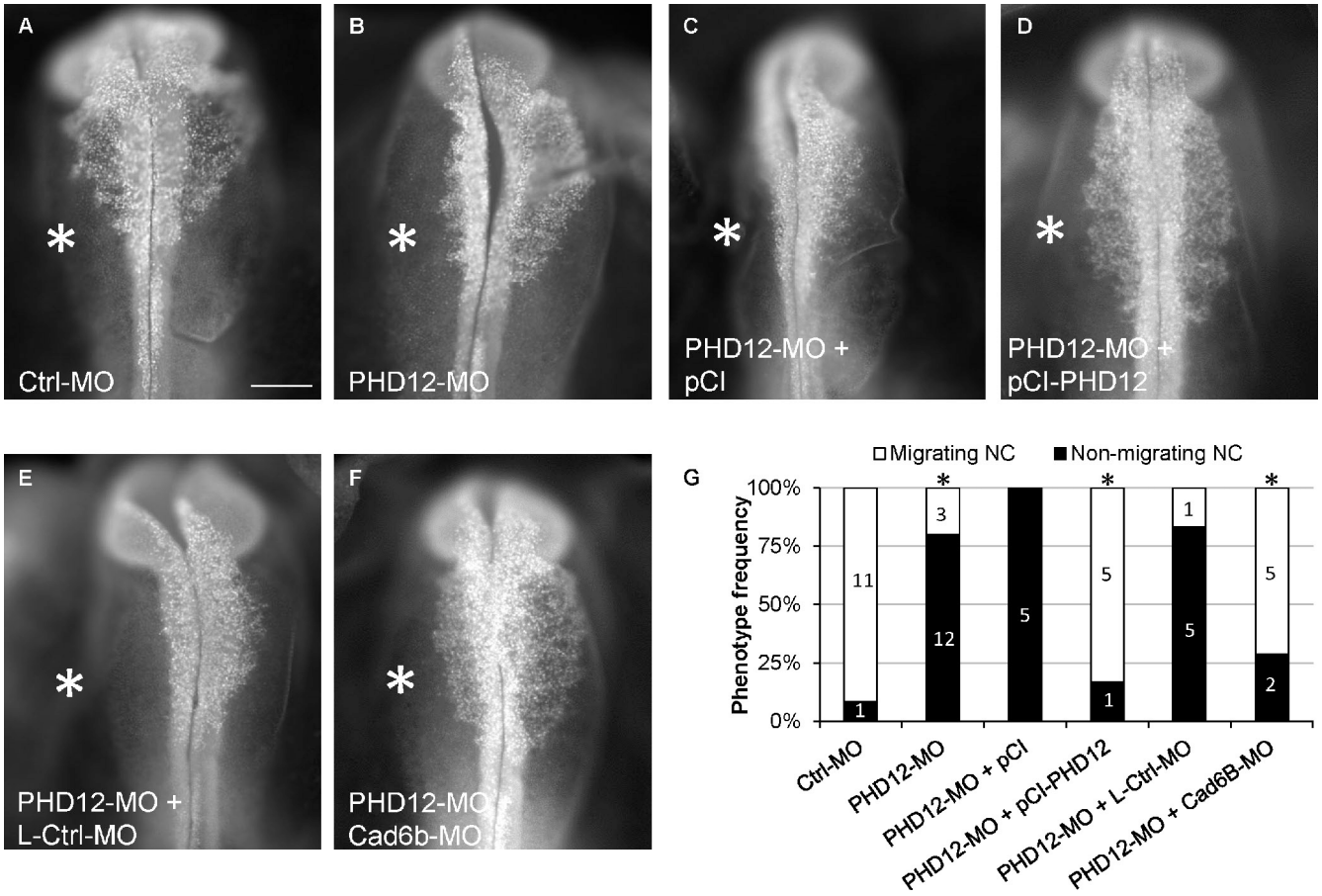

Figure 5. **Coelectroporation of PHD12 mRNA or Cad6b morpholino rescues the lack of neural crest EMT caused by loss of PHD12.** (A and B) Electroporation of PHD12-MO into the left side of the embryo (asterisks) causes a drastic reduction in the numbers of FoxD3-positive migrating neural crest cells compared with the uninjected side or with Ctrl-MO–treated embryo as assayed by immunohistochemistry. (C and D) Coelectroporation of PHD12-MO together with a vector containing the coding region of PHD12 (pCI-PHD12) restores the numbers of migrating FoxD3-positive neural crest cells. In contrast, coelectroporation of PHD12-MO plus an empty vector (pCI) fails to rescue the loss-of-function phenotype. (E and F) Coelectroporation of PHD12-MO together with a Cad6b-MO restores the migration of FoxD3-positive neural crest cells, whereas coelectroporation with control morpholino (L-Ctrl-MO) does not. (G) Quantitation of the phenotype based on the presence or absence of FoxD3-positive migrating neural crest cells compared with the contralateral side of the embryo. Asterisks indicate significant differences ($P < 0.05$) compared with each specific control by contingency table followed by χ^2 test. Numbers represent analyzed embryos. Bar, 100 µm.

embryos at the 9ss stage, by which time neural crest emigration has initiated. Confocal images showed persistence of Cad6b protein expression at the midbrain level on the PHD12-MO–treated side compared with the uninjected side (Fig. 4, A–C), suggesting that cells have increased levels of adhesion and fail to become mesenchymal. Moreover, double staining with antibodies to Cad6b and FoxD3 on morpholino-treated embryos revealed retention of Cad6b expression in the dorsal neural tube that colocalizes with FoxD3-positive cells that appear unable to migrate (Fig. 4, D–I), as quantified in Fig. 4. The results show that PHD12 protein knockdown significantly ($P < 0.01$) affects the ability of neural crest cells to undergo EMT and become mesenchymal (13/15 embryos), when compared with Ctrl-MO–treated embryos (1/12 embryos).

To better distinguish between a failure in EMT versus lack of motility of neural crest cells, we turned to in vitro experiments in which neural tube explants were electroporated with PHD12-MO on one side and then examined for the subsequent ability of neural crest cells to migrate. The results reveal a near complete lack of emigrating neural crest cells on the PHD12 morpholino electroporated side compared with untreated side or with the Ctrl-MO–treated explants (Fig. S3). Rather than affecting motility, the results suggest that there is a specific effect on EMT via retention of Cad6b expression that prevents emigration and acquisition of mesenchymal, migratory morphology.

To control for the specificity of our morpholino knockdown, rescue experiments were performed in which we coelectroporated PHD12-MO with a vector encoding full-length PHD12 protein (pCI-PHD12) plus nuclear RFP as a marker (Fig. 5). Coelectroporation of morpholino plus rescue construct resulted in a significant reduction ($P < 0.05$) in the severity of the phenotype compared with coelectroporation of PHD12-MO plus empty vector (pCI). In addition, coelectroporation of PHD12-MO (FITC labeled) and Cad6b-MO (lysamine labeled) also significantly rescued ($P < 0.05$) the phenotype, restoring neural crest migration. In contrast, coelectroporation with lysamine-labeled Ctrl-MO (L-Ctrl-MO) failed to increase the numbers of FoxD3-positive migrating neural crest cells. These results confirm that PHD12 protein is involved in neural crest EMT rather than initial specification.

Published September 17, 2012

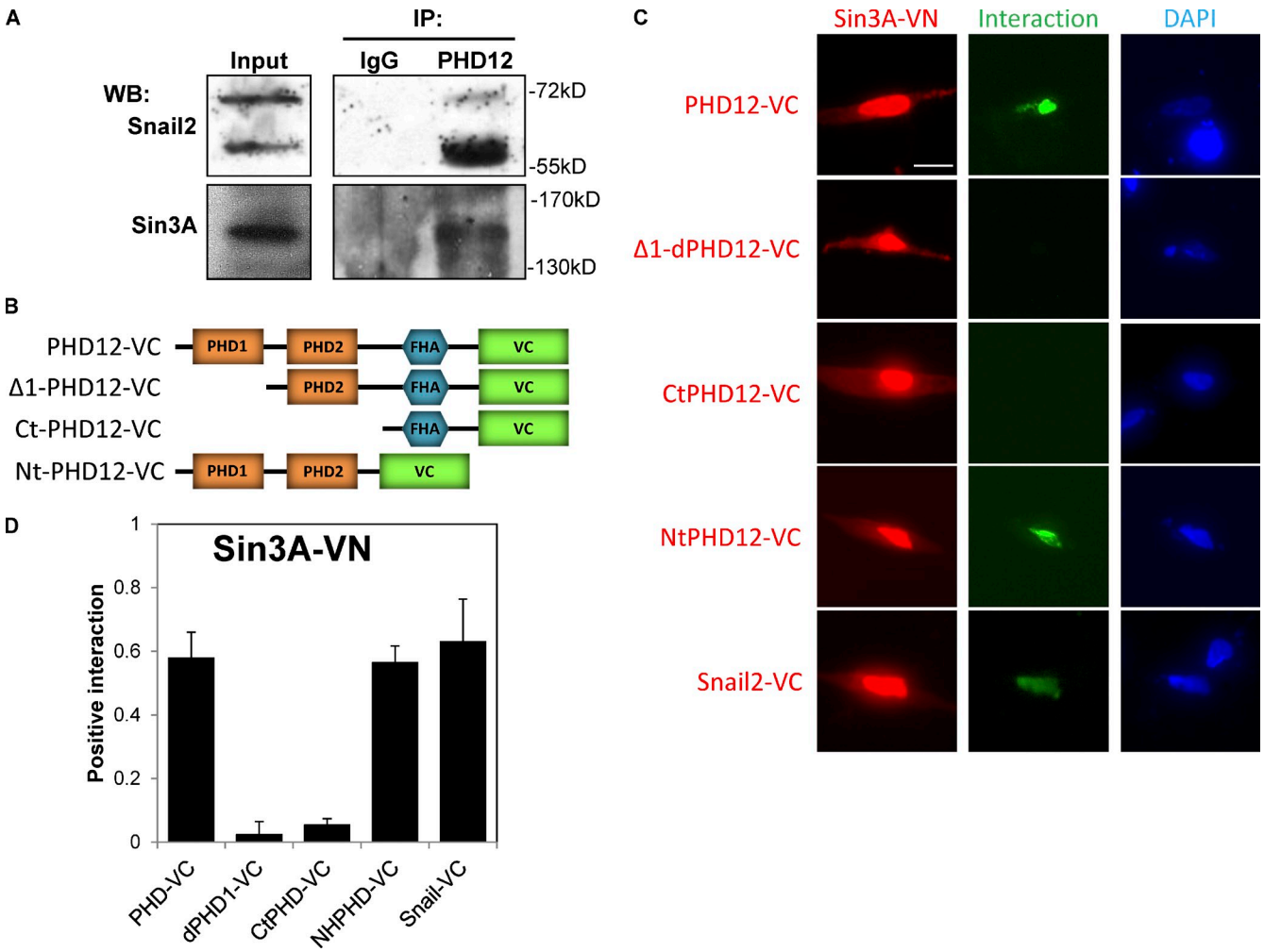

Figure 6. **PHD12 protein interacts in vivo with Sin3A and indirectly with Snail2 as revealed by co-IP and BiFC.** (A) Western blots using anti-Snail2 and -Sin3A on PHD12 or IgG immunoprecipitates (IP) from dorsal neural tubes from 6–8ss embryos. Input represent 0.1% of each IP. (B) Schematic representation of PHD12 constructs used for the bimolecular fluorescence complementation (BiFC) assay. (C and D) Visualization and quantification of BiFC on chick fibroblast transfected with PHD12 and truncated PHD12, Snail2, and Sin3A fused to the C or N terminus of Venus protein. Y axis on graph represents the fraction of transfected cells in which Venus fluorescence was visualized. Ct, C terminus; Nt, N terminus; FHA, Forkhead-associated domain; VC, Venus C terminus; VN, Venus N terminus; WB, Western blot. Error bars show SDs. Bar, 16 µm.

To look at long-term effects of the PHD12 depletion, we examined the formation of the trigeminal, geniculate, and petrosal peripheral ganglia of the head, which receive an important contribution from the neural crest (Fig. S4). The results show a severe defect in ganglion formation, particularly evident in the trigeminal ganglion, the largest of the cranial ganglia, which appears smaller and malformed on the injected side of PHD12-MO–treated embryos compared with the uninjected side of the same embryo or with Ctrl-MO–treated embryos. Collectively, these results show that interfering with PHD12 function during neural crest EMT causes profound later defects in neural crest derivatives.

PHD12 protein interacts in vivo with Sin3A and indirectly with Snail2

To characterize the molecular interaction of PHD12, Snail2, and Sin3A, we performed an in vivo coimmunoprecipitation (IP; co-IP) assay using 100 dorsal neural tubes carefully dissected from embryos at 7–9ss. The results show that endogenous PHD12 protein co-IPs with both Snail2 and Sin3A, as revealed by Western blot analysis (Fig. 6 A). These results clearly demonstrate that PHD12 is able to interact with both Snail2 and the Sin3A repressive complex.

To distinguish whether this interaction is direct or indirect, we used bimolecular fluorescence complementation (BiFC), a powerful technique allowing protein interactions to be visualized within living cells. To this end, we generated full-length or truncated PHD12, Snail2, and Sin3A coupled to the Venus N terminus or C terminus domains (Fig. 6, B–D). After transfection of these constructs into chick fibroblasts, Venus signal (Fig. 6, green) is detectable only when two proteins interact. Interestingly, the results show that PHD12 protein directly interacts with Sin3A via its N terminus containing two PHD domains. In contrast, the C terminus containing the Forkhead-associated domain does not interact with Sin3A. Conversely, Snail2 does not directly interact with PHD12 (unpublished data) but rather interacts with Sin3A. These results not only reveal the mechanisms underlying the binding of PHD12 but also demonstrate that Sin3A forms a molecular bridge within this complex.

Published September 17, 2012

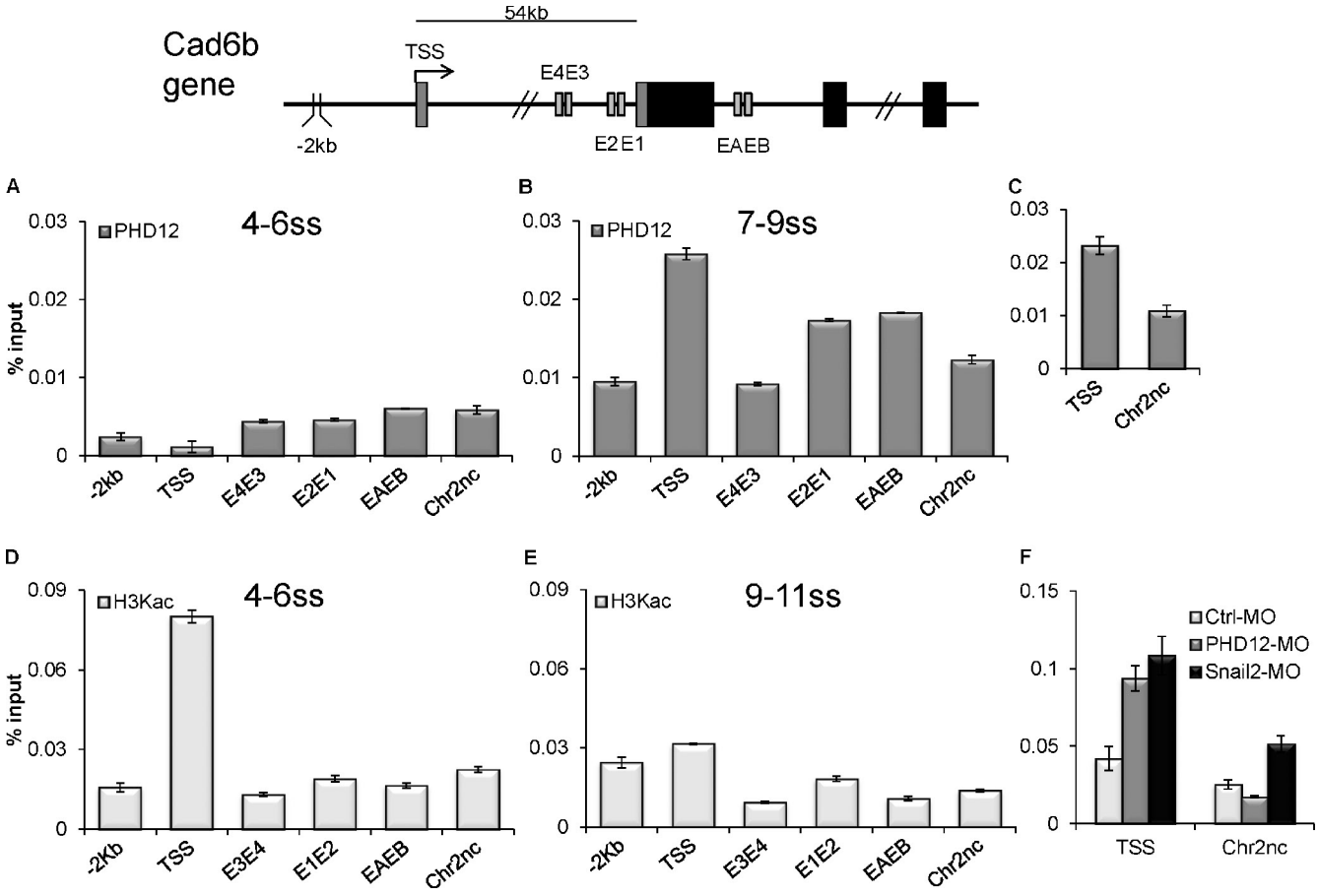

Figure 7. **Endogenous PHD12 is recruited to the Cad6b promoter in vivo and is accompanied by histone 3 lysine deacetylation, correlating with the gene repression before neural crest EMT.** ChIP assays were used to assess PHD12 binding and H3KAc to the Cad6b locus at different developmental stages. Two independent experiments were performed using 30 dorsal neural tubes for each stage. The vertical axis represents percentage of input (ChIP enriched/input), and horizontal axis represents different positions on the Cad6b locus. Schematic diagrams at top represent primer locations −2 kb from the transcription start site (TSS), the TSS, and the different E-boxes over the Cad6b gene. One representative sample is depicted per stage. (A) The results show no association of PHD12 on any analyzed regions of Cad6b at 4–5ss when compared with a distant, intergenic control region of the same chromosome 2 (Chr2nc). (B) In contrast, there is consistent PHD12 association with the Cad6b TSS at 7–9ss. (C) We also observed enhanced association using a different set of primers located at the Cad6b TSS. (D) H3Kac analysis shows high association at the TSS of Cad6b at 4–5ss but not in the other analyzed regions or the Chr2nc. (E) At 9–11ss, the H3KAc has low association values in all analyzed regions of Cad6b and the Chr2nc. (F) ChIP assay performed on 12 dorsal neural tube from PHD12-MO– and Snail2-MO–treated embryos sampled at 9–10ss shows a lack of deacetylation of the TSS of Cad6b gene compared with Ctrl-MO–treated embryos. See also Fig. S5 including IgG ChIP. Error bars show SDs.

PHD12 is recruited to the Cad6b promoter in vivo

To demonstrate in vivo association of PHD12 protein with the putative Cad6b regulatory region, we performed in vivo chromatin IP (ChIP) experiments in conjunction with QPCR on midbrain dorsal neural tubes from embryos at different stages (Fig. 7, A–C; and Fig. S5). At early stages (4–6ss), before normal neural crest EMT, we failed to detect association of PHD12 protein with the Cad6b regulatory regions, relative to negative controls situated in ORF-free intergenic regions on the same chromosome (Chr2nc [chromosome 2 negative control]). However, at 7–9ss, which correlates with the onset of EMT, enhanced PHD12 interaction was observed on the transcription start site (TSS) and E-boxes (E2E1/EAEB boxes) of Cad6b. These data demonstrate that PHD12 interacts in vivo in a time- and location-dependent manner with Cad6b and are consistent with the possibility that PHD12 may be involved in Cad6b repression before neural crest EMT.

Histone acetylation regulates Cad6b expression in vivo

Based on the premise that PHD12 together with Snail2 are recruited to the Cad6b locus and also interact with the Sin3A repressive complex, we examined the level of histone acetylation as a possible basis for Cad6b repression. To this end, we analyzed the presence of acetylated lysines on histone 3 (H3Kac) by ChIP QPCR on Cad6b regulatory regions using dorsal neural tubes from 4–6ss and 9–11ss embryos (Fig. 7, D and E; and Fig. S5). The results revealed a hyperacetylated region on the TSS at stage 4–6ss, before neural crest migration, which is removed by stage 9–11ss after neural crest cells undergo EMT. In contrast, after morpholino-mediated loss of PHD12 or Snail2, histone 3 hyperacetylation at the TSS of the Cad6b promoter persists at the 9–10ss stage (Fig. 7 F). Based on these findings, we propose a model illustrated in Fig. 8, in which a loop in the Cad6b locus brings together two regulatory regions, one located on the promoter, where PHD12 is

Published September 17, 2012

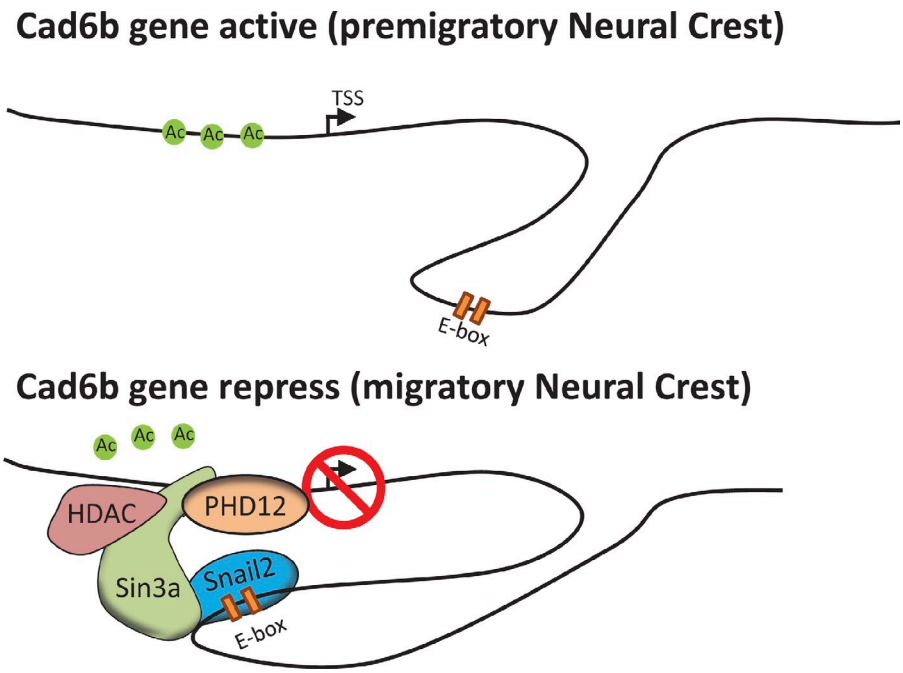

Figure 8. **Schematic model.** The results suggest a model in which PHD12 and Snail2 associate with the TSS and E-boxes, respectively, on the Cad6b gene to recruit the Sin3A–HDAC repressive complex. This interaction allows the subsequent deacetylation of histone H3 at the promoter of the Cad6b gene, resulting in repression of its transcription. This in turn allows neural crest EMT. Ac, acetylation.

recruited, and the other on the E-boxes, were Snail2 binds, with Sin3A–HDAC acting as a molecular bridge between PHD12 and Snail2.

Discussion

The EMT is a carefully controlled event that occurs often during developmental processes and reappears in the adult during tumor metastasis. EMT is characterized by a loss of cell polarity and is strictly regulated spatially and temporally (Cano et al., 2000; Bolós et al., 2003; Côme et al., 2004). In vivo and in vitro experiment have identified Snail family members as important regulators of this process, functioning by directly binding to Snail binding sites (E-boxes) in the E-cadherin promoter to repress its transcription (Batlle et al., 2000; Cano et al., 2000). In the neural crest, Snail2 has been shown to bind to the Cad6b locus and repress its expression before EMT (Taneyhill et al., 2007). However, the molecular machinery mediating this repression was largely unknown.

Here, we show that before neural crest EMT, the adaptor protein PHD12 is expressed in the dorsal neural tube from which neural crest cells emigrate. PHD12 interacts with Sin3A that in turn interacts with Snail2, recruiting the complex to the Cad6b regulatory region. This results in a dramatic histone H3 deacetylation on the Cad6b TSS. Accordingly, we postulate a model (Fig. 8) in which a loop in the Cad6b locus brings together two regulatory regions, one located on the promoter, where PHD12 is recruited, and the other on the E-boxes, where Snail2 binds (Taneyhill et al., 2007). By binding to both PHD12 and Snail2, the Sin3A–HDAC repressive complex forms a molecular bridge and deacetylates histone H3 at the Cad6b promoter to repress its expression. This dual specificity of epigenetic and transcriptional marks confers an additional fine level of regulation to the neural crest EMT.

Our multiplex NanoString data reveal that PHD12 is required for repression of both Cad6b and E-cadherin. The persistence of Cad6b expression after PHD12 knockdown in turn results in abrogation of neural crest emigration, maintaining the neural crest cells as adherent rather than mesenchymal cells. Although E-cadherin is normally expressed only in the ectoderm rather than the dorsal neural tube, its ectopic expression in the dorsal neural tube after PHD12 knockdown is similar to that observed after loss of the EMT gene Zeb2 in mouse embryos (Van de Putte et al., 2003), which causes a retention of E-cadherin in the dorsal neural tube. In addition to direct effects, PHD12 knockdown also indirectly affects other gene products. For example, we observed a slight increase in the *PERP* after loss of PHD12, perhaps reflecting the possibility that cells incapable of undergoing EMT may enter an apoptotic pathway. In addition, we noted a consistent up-regulation of SFRP1, which acts as a decoy receptor modulating Wnt signaling. Secreted frizzled-related proteins play an important role in many vertebrate tissues (Leimeister et al., 1998; Esteve et al., 2000; Chapman et al., 2004), including the neural crest; mice lacking both SFRP1/SFRP2 exhibit a significant neural crest defect (Misra and Matise, 2010). Similar to embryonic tissues, in many cancers, epigenetic silencing of SFRP1 leads to inappropriate activation of the Wnt pathway (Klopocki et al., 2004; Huang et al., 2007; Kongkham et al., 2010; Lee et al., 2010). Moreover, blocking Wnt signaling by secreted frizzled-related protein–like molecules in vivo inhibits cell proliferation and tumor growth (Lavergne et al., 2011).

Our results demonstrate a direct interaction between PHD12 and the corepressor Sin3A, which in turn binds to Snail2, to repress Cad6b via promoter deacetylation. PHD motifs are known to cooperate with the adjacent bromodomain, such as those found in PHD12, to confer a robust association with native hyperacetylated nucleosomes (Bienz, 2006), characteristic of transcriptionally active genes. Similarly, we find that the Cad6b promoter transitions from hyperacetylated at the 4–6ss to hypoacetylated at 10–11ss. This reflects a change

Published September 17, 2012

from active to inactive Cad6b transcription, in preparation for neural crest EMT. Recently, the PHD domain also has been shown to bind to the tail of histone H3 that is trimethylated on lysine 4 (Mellor, 2006; Peña et al., 2006), a characteristic epigenetic mark of transcriptionally active genes. Collectively, with our ChIP results, this suggests that a hyperacetylated region together with H3K4me3 may serve as anchors for interaction with PHD12.

Based on the cumulative results, we hypothesize that PHD12 is a necessary partner for consolidating and/or strengthening the association of a repressive complex with a specific chromatin structure. This model (Fig. 8) explains why both PHD12 and Snail2 are required to read the epigenetic mark and DNA sequence (E-boxes), respectively. We propose that both PHD12 and Snail2 work cooperatively to recruit Sin3A–HDAC to repress the target gene via deacetylation. Consistent with this possibility, we show that both PHD12 and Snail2 directly interact with Sin3A. This dual specificity may underlie the fine tuning that controls the timing of changes responsible for the neural crest EMT in vivo. These results reveal for the first time the nature of the complex regulating neural crest EMT. The similarities between neural crest EMT and tumor metastasis raise the intriguing possibility that related complexes may be involved in regulating other EMTs, such as those occurring during cancer progression.

Materials and methods

Embryos

Fertilized chicken (*Gallus gallus domesticus*) eggs were obtained from local commercial sources and incubated at 37°C to the desired stages according to the criteria of Hamburger and Hamilton.

RNA preparation and QPCR

RNA was prepared from individual embryos ($n = 3$) using an isolation kit (RNAqueous-Micro; Ambion) following the manufacturer's instruction. The RNA was treated with amplification grade DNaseI (Invitrogen) and then reversed transcribed to cDNA with a reverse transcription kit (SuperScript III; Invitrogen) using random hexamers. QPCR was performed using a 96-well plate QPCR machine (ABI 7000; Applied Bioscience) in a TaqMan assay (Applied Biosciences) with SYBR green with 6-carboxy-X-rhodamine (SYBR green iTaq Supermix; Bio-Rad Laboratories), 150–450 nM of each primer, and 200–500 ng cDNA in a 25-µl reaction volume. During the exponential phase of the QPCR reaction, a threshold cycle and baseline were set according to the protocols of Applied Biosystems. The results for different samples were interpolated on a line created by running standard curves for each primer set and then normalized against the glyceraldehyde 3-phosphate dehydrogenase housekeeping gene. These calculations were performed according to the standard curve assay method that is detailed in the Applied Biosystems protocols. Three replicates were loaded of every sample and points of the standard curve.

Electroporation of antisense morpholinos and vectors

Two antisense morpholinos to PHD12 were designed, one near the ATG codon (5′-TCGTCTC**CAT**CTTCTCCACATTCAT-3′; bold letters correspond to the ATG codon) and the second located at the second exon–intron boundary (5′-GGGAGCGCGGAGCCTTACCAGCACT-3′), both yielding similar results. Injections of fluorescein-tagged morpholino (0.75 mM plus 0.3 ng plasmidic DNA used as a carrier) and pCI-H2BRFP and pCI-PHD12-H2BRFP vectors were performed by air pressure using a glass micropipette targeted to the presumptive neural crest region at stages 4–5. Electroporations at stages 4–5 were performed on whole-chick embryo explants placed ventral side up on filter paper rings. The morpholinos and vectors were injected on the left side of the embryo, and platinum electrodes were placed vertically across the chick embryos and electroporated with five pulses of 5.5 V for 50 ms at 100-ms intervals. Embryos were cultured in 0.5 ml albumen in tissue-culture dishes until the desired stages. Embryos were then removed and fixed overnight in 4% PFA at 4°C. They were then placed in PBS, viewed, and photographed as whole mounts using a fluorescence stereomicroscope (Discovery V12; Carl Zeiss) to determine electroporation efficiency. Embryos used for in situ hybridization (ISH) were dehydrated in a MeOH/PTW (PBS with Tween) series at room temperature before being stored at −20°C in 100% MeOH.

ISH

Whole-mount ISH was performed as described previously (Kee and Bronner-Fraser, 2001). Digoxigenin-labeled probes were synthesized from the full-length chicken cDNA of PHD12, Snail2, and FoxD3 using linearized plasmid. Hybridized probes were detected using an alkaline phosphatase–conjugated antidigoxigenin antibody (1:2,000; Roche) in the presence of nitro blue tetrazolium/5-bromo-4-chloro-3′-indolyphosphate substrates (Roche). Whole-mount pictures were taken using AxioVision software (Carl Zeiss) with a microscope (Stemi SVII; Carl Zeiss). Some embryos were fixed in 4% PFA in PBS, washed, embedded in gelatin, and cryostat sectioned at a thickness of 16 µm. They were photographed using the AxioVision software with a microscope (Axioskop 2 Plus; Carl Zeiss) and processed using Photoshop (CS3; Adobe).

nCounter

Individual half-dorsal neural tubes (injected vs. uninjected) were carefully dissected from four 9–10ss embryos that had been treated with Ctrl-MO or PHD12-MO. The tissue was disaggregated in lysis buffer (Ambion) and stored at −80°C. The total RNA from each lysate was hybridized with the capture and reporter probes, custom designed for multiplex detection of 70 genes, and incubated overnight at 65°C according to the nCounter Gene Expression Assay manual. All posthybridization steps were handled robotically by a custom liquid-handling robot. After the washes, the purified target–probe complexes were eluted off and immobilized in the cartridge for data collection performed in the nCounter Digital Analyzer. Data were normalized to the total counts obtained on each side of the embryo in each sample.

Whole-mount immunohistochemistry

Whole-mount chick immunohistochemistry was performed as previously described (Taneyhill et al., 2007). In brief, embryos were fixed for 15 min in 4% PFA and then permeabilized and blocked in TBS (500 mM Tris-HCl, pH 7.4, 1.5 M NaCl, and 10 mM $CaCl_2$) containing 0.1% Triton X-100 (PBS-T) and 5% FBS for 60 min at room temperature. Primary antibodies were diluted in TBS-T/FBS and incubated overnight at 4°C. Primary antibodies used were mouse anti-Snail2 (1:500), anti-Cad6b (1:100; all supplied by the Developmental Studies Hybridoma Bank), and rabbit anti-FoxD3 (1:500; gift of P. Labosky, Vanderbilt University Medical Center, Nashville, TN). Secondary antibodies used were goat anti–mouse and anti–rabbit Alexa Fluor 350 and 594 (1:1,000; all obtained from Molecular Probes) diluted in TBS-T/FBS and incubated for 45 min at room temperature. All washes were performed in TBS-T at room temperature. Some embryos were subsequently embedded in gelatin, cryostat sectioned at 16 µm, coverslipped using Permafluor (Beckman Coulter), photographed using the AxioVision software with a fluorescence microscope (Axioskop 2 Plus), and processed using Photoshop CS3.

In vitro neural tube culture

Chick embryos were electroporated on one side with either PHD12-MO or Ctrl-MO. At stage 9, the neural tubes at the midbrain level were carefully excised and explanted onto fibronectin-coated 8-well slides. Explants were cultured in Ham's F12 medium with L-glutamine (Gibco) media containing 1% N2 supplement (Gibco) and 1% penicillin-streptomycin (Gibco) for 16 h at 37°C and 5% CO_2. Subsequently, the cultures were fixed for 15 min in 4% PFA, DAPI stained, and photographed as described in the immunohistochemistry methodology.

ChIP

Dorsal neural tubes from 30 embryos were dissected from two independent experiments at stages 5–6ss, 7–9ss, and 10–11ss and homogenized in nuclei extraction buffer (0.25% NP-40, 0.25% Triton X-100, 10 mM Tris-HCl, pH 7.5, 3 mM $CaCl_2$, 0.25 M sucrose, 1 mM DTT, 0.2 mM PMSF, and EDTA-free protease inhibitor [Complete; Roche]). Cells were cross-linked with 1% formaldehyde for 10 min at room temperature, and formaldehyde was then inactivated by the addition of 125 mM glycine for 5 min. Cross-linked cells were centrifuged, and the pellet was washed three times in cold PBS containing protease inhibitor. The final pellet was snap frozen in liquid nitrogen and stored at −80°C until use. Cells were resuspended in 1 ml nuclei extraction buffer and rehomogenized until the nuclei went into the solution. After centrifugation, the pellet was resuspended in SDS-lysis

Published September 17, 2012

buffer (1% SDS, 50 mM Tris, pH 8.0, 10 mM EDTA, and EDTA-free protease inhibitors), and 2 vol ChIP dilution buffer (0.01% SDS, 1.2 mM EDTA 16.7 mM Tris-Cl, pH 8.0, 167 mM NaCl, 1 mM DTT, 0.2 mM PMSF, and stock of Complete EDTA-free protease inhibitor) was added. Chromatin was sheared to 300–800-bp fragments using a sonicator (Amp: 5 and 30 s on and 1 min off for 6-min process time) and centrifuged, and the supernatant was split in three tubes for input sample, mock control (rabbit anti-IgG), and target antibodies of anti-H3Kac (EMD Millipore) and/or anti-Pf1/PHD12 (Novus Biologicals) all bound to protein A magnetic beads (Invitrogen). IgG and target antibodies (10 µg) were incubated nutating overnight at 4°C and after extensive washes with radioimmunoprecipitation assay buffer (50 mM Hepes-KOH, pH 8, 500 mM LiCl, 1 mM EDTA, 1% NP-40, 0.7% Na-deoxycholate, 1 mM DTT, 0.2 mM PMSF, and a stock of Complete protease inhibitor), and the complexes were resuspended in elution buffer (50 mM Tris-HCl, pH 8.0, 10 mM EDTA, and 1% SDS). The magnetic beads were eluted by incubating at 65°C for 15 min, vortexing every 2 min, and then spun down at 16,000 *g* for 1 min at room temperature. The supernatant was reverse cross-linked by heating at 65°C on. Immunoprecipitated DNA was treated with 0.2 µg/ml RNase A and 0.2 µg/ml proteinase K both for 1 h. Phenol/chloroform/isoamyl alcohol extraction was performed followed by EtOH precipitation. Finally, the obtained DNA was used as a template for QPCR analyses. Every sample was loaded as three replicates each and expressed as percentage of input.

Co-IP

Two independent experiments were performed using nuclear protein extracted from 100 dorsal neural tubes dissected from 7–9ss embryos in ice-cold hypotonic lysis buffer (100 mM Hepes, pH 7.9, 15 mM $MgCl_2$, 100 mM KCl, 0.5 mM DTT, EDTA-free protease inhibitors, and 0.2 mM PMSF) using a dounce homogenizer. The nuclear pellet was resuspended in extraction buffer (20 mM Hepes, pH 7.9, 0.42 M NaCl, 1.5 mM $MgCl_2$, 0.2 mM EDTA, 25% glycerol, EDTA-free protease inhibitors, and 0.2 mM PMSF) and passed 10 times through a syringe needle to disrupt the nuclear wall. The nuclear suspension was centrifuged at 21,000 *g* for 5 min at 4°C, and one fifth of the supernatant was saved as input. The remaining sample was combined with the rabbit anti-PHD12 and anti-IgG (150–300 µg nuclear protein per 10–20 µg antibody), previously cross-linked to the magnetic beads using Dynabeads M-280 Tosylactivated (Invitrogen) following the manufacturer's directions and incubated for 2 h at 4°C. The endogenous protein complexes were magnetically isolated, washed several times with modified radioimmunoprecipitation assay buffer (50 mM Tris-HCl, pH 7.4, 1% NP-40, 0.25% Na-deoxycholate, 150 mM NaCl, 1 mM EDTA, 1 mM PMSF, 1mM DTT, and protease inhibitors), and eluted in SDS sample buffer. Finally, an SDS-PAGE followed by Western blotting was performed using rabbit anti-Sin3A (1:1,000; Abcam) and mouse anti-Snail2 (1:500) antibodies. 0.1% of the IP sample was used as the input.

BiFC

The BiFC vectors (provided by C.-D. Hu, University School of Pharmacy, West Lafayette, IN) containing the N- and C-terminal halves of Venus (aa 1–172 and 173–239) were cloned in pCI vectors containing an internal ribosome entry site followed by membrane RFP or nuclear H2BRFP as reporters of transfection efficiency. Full-length and truncated PHD12, Snail2, and Sin3A were cloned in frame upstream of the Venus halves. Chicken fibroblast cells were transfected following standard protocol. In brief, cells were grown to near confluence in serum-rich media (10% FBS, 2% chicken serum, and 1% L-glutamine in high glucose DME) containing penicillin/streptomycin antibiotics. Cells were washed in DME and trypsinized for 1 min, and 10 ml serum-rich media was added to stop trypsinization. Cells were placed into 8-well fibronectin-coated slides and incubated until 60–80% confluency. Before transfection, media were rinsed off, cells were washed with DME, and finally, enriched DME (1% L-glutamine and nonessential amino acids) was added. Vectors were combined with Lipofectamine (Invitrogen) in Opti-MEM and added to the cells. After 6 h, the media were replaced with serum-rich media, and the cells were visualized the next day by epifluorescence on a compound fluorescence microscope as described in the immunohistochemistry methodology. The percentage of Venus-positive cells from 100 transfected cells was analyzed in quadruplicate in two independent experiments.

Online supplemental material

Fig. S1 shows the effect of both PHD-spMO and PHD12-tMO on the PHD12 mRNA and protein levels, respectively. Fig. S2 shows that PHD12-MO does not affect the expression of FoxD3 and Snail2 in premigratory neural crest cells. Fig. S3 shows the lack of neural crest migration on neural tube explant treated with PHD12-MO. Fig. S4 shows the long-term effect of PHD12 depletion in cranial ganglia formation. Fig. S5 shows the ChIP IgG control presented in Fig. 7. Online supplemental material is available at http://www.jcb.org/cgi/content/full/jcb.201203098/DC1.

We are indebted to Dr. Tatjana Sauka-Spengler for her help and advice throughout this project and for the final design of the BiFC vectors to work in chick cells. We are grateful to Dr. Chang-Deng Hu and Dr. Patricia Labosky for kindly providing invaluable reagents of the BiFC vectors and FoxD3 antibody, respectively, as well as Joanna Tan-Cabuga for excellent technical assistance.

This work was supported by DE16459 and HD037105 grants to M.E. Bronner and a Fogarty grant R03 DE022521 to M.E. Bronner and P.H. Strobl-Mazzulla.

Submitted: 19 March 2012
Accepted: 21 August 2012

References

Adams, M.S., L.S. Gammill, and M. Bronner-Fraser. 2008. Discovery of transcription factors and other candidate regulators of neural crest development. *Dev. Dyn.* 237:1021–1033. http://dx.doi.org/10.1002/dvdy.21513

Barrallo-Gimeno, A., and M.A. Nieto. 2005. The Snail genes as inducers of cell movement and survival: implications in development and cancer. *Development*. 132:3151–3161. http://dx.doi.org/10.1242/dev.01907

Batlle, E., E. Sancho, C. Francí, D. Domínguez, M. Monfar, J. Baulida, and A. García De Herreros. 2000. The transcription factor snail is a repressor of E-cadherin gene expression in epithelial tumour cells. *Nat. Cell Biol.* 2: 84–89. http://dx.doi.org/10.1038/35000034

Bienz, M. 2006. The PHD finger, a nuclear protein-interaction domain. *Trends Biochem. Sci.* 31:35–40. http://dx.doi.org/10.1016/j.tibs.2005.11.001

Bolós, V., H. Peinado, M.A. Pérez-Moreno, M.F. Fraga, M. Esteller, and A. Cano. 2003. The transcription factor Slug represses E-cadherin expression and induces epithelial to mesenchymal transitions: a comparison with Snail and E47 repressors. *J. Cell Sci.* 116:499–511. http://dx.doi.org/10.1242/jcs.00224

Cano, A., M.A. Pérez-Moreno, I. Rodrigo, A. Locascio, M.J. Blanco, M.G. del Barrio, F. Portillo, and M.A. Nieto. 2000. The transcription factor snail controls epithelial-mesenchymal transitions by repressing E-cadherin expression. *Nat. Cell Biol.* 2:76–83. http://dx.doi.org/10.1038/35000025

Chapman, S.C., R. Brown, L. Lees, G.C. Schoenwolf, and A. Lumsden. 2004. Expression analysis of chick Wnt and frizzled genes and selected inhibitors in early chick patterning. *Dev. Dyn.* 229:668–676. http://dx.doi.org/10.1002/dvdy.10491

Côme, C., V. Arnoux, F. Bibeau, and P. Savagner. 2004. Roles of the transcription factors snail and slug during mammary morphogenesis and breast carcinoma progression. *J. Mammary Gland Biol. Neoplasia*. 9:183–193. http://dx.doi.org/10.1023/B:JOMG.0000037161.91969.de

Esteve, P., J. Morcillo, and P. Bovolenta. 2000. Early and dynamic expression of cSfrp1 during chick embryo development. *Mech. Dev.* 97:217–221. http://dx.doi.org/10.1016/S0925-4773(00)00421-4

Fortina, P., and S. Surrey. 2008. Digital mRNA profiling. *Nat. Biotechnol.* 26:293–294. http://dx.doi.org/10.1038/nbt0308-293

Hatta, K., S. Takagi, H. Fujisawa, and M. Takeichi. 1987. Spatial and temporal expression pattern of N-cadherin cell adhesion molecules correlated with morphogenetic processes of chicken embryos. *Dev. Biol.* 120:215–227. http://dx.doi.org/10.1016/0012-1606(87)90119-9

Hemavathy, K., S.I. Ashraf, and Y.T. Ip. 2000. Snail/slug family of repressors: slowly going into the fast lane of development and cancer. *Gene*. 257: 1–12. http://dx.doi.org/10.1016/S0378-1119(00)00371-1

Huang, J., Y.L. Zhang, X.M. Teng, Y. Lin, D.L. Zheng, P.Y. Yang, and Z.G. Han. 2007. Down-regulation of SFRP1 as a putative tumor suppressor gene can contribute to human hepatocellular carcinoma. *BMC Cancer*. 7: 126. http://dx.doi.org/10.1186/1471-2407-7-126

Kee, Y., and M. Bronner-Fraser. 2001. Temporally and spatially restricted expression of the helix-loop-helix transcriptional regulator Id1 during avian embryogenesis. *Mech. Dev.* 109:331–335. http://dx.doi.org/10.1016/S0925-4773(01)00574-3

Klopocki, E., G. Kristiansen, P.J. Wild, I. Klaman, E. Castanos-Velez, G. Singer, R. Stöhr, R. Simon, G. Sauter, H. Leibiger, et al. 2004. Loss of SFRP1 is associated with breast cancer progression and poor prognosis in early stage tumors. *Int. J. Oncol.* 25:641–649.

Kongkham, P.N., P.A. Northcott, S.E. Croul, C.A. Smith, M.D. Taylor, and J.T. Rutka. 2010. The SFRP family of WNT inhibitors function as novel tumor suppressor genes epigenetically silenced in medulloblastoma. *Oncogene*. 29:3017–3024. http://dx.doi.org/10.1038/onc.2010.32

Lavergne, E., I. Hendaoui, C. Coulouarn, C. Ribault, J. Leseur, P.A. Eliat, S. Mebarki, A. Corlu, B. Clément, and O. Musso. 2011. Blocking Wnt signaling by SFRP-like molecules inhibits in vivo cell proliferation and tumor growth in cells carrying active β-catenin. *Oncogene*. 30:423–433. http://dx.doi.org/10.1038/onc.2010.432

Le Douarin, N.M., and C. Kalcheim. 1999. The neural crest. Second edition. Cambridge University Press, Cambridge, UK/New York. 445 pp.

Lee, C.H., Y.J. Hung, C.Y. Lin, P.H. Hung, H.W. Hung, and Y.S. Shieh. 2010. Loss of SFRP1 expression is associated with aberrant beta-catenin distribution and tumor progression in mucoepidermoid carcinoma of salivary glands. *Ann. Surg. Oncol.* 17:2237–2246. http://dx.doi.org/10.1245/s10434-010-0961-z

Leimeister, C., A. Bach, and M. Gessler. 1998. Developmental expression patterns of mouse sFRP genes encoding members of the secreted frizzled related protein family. *Mech. Dev.* 75:29–42. http://dx.doi.org/10.1016/S0925-4773(98)00072-0

Mellor, J. 2006. It takes a PHD to read the histone code. *Cell*. 126:22–24. http://dx.doi.org/10.1016/j.cell.2006.06.028

Misra, K., and M.P. Matise. 2010. A critical role for sFRP proteins in maintaining caudal neural tube closure in mice via inhibition of BMP signaling. *Dev. Biol.* 337:74–83. http://dx.doi.org/10.1016/j.ydbio.2009.10.015

Nakagawa, S., and M. Takeichi. 1995. Neural crest cell-cell adhesion controlled by sequential and subpopulation-specific expression of novel cadherins. *Development*. 121:1321–1332.

Nieto, M.A. 2002. The snail superfamily of zinc-finger transcription factors. *Nat. Rev. Mol. Cell Biol.* 3:155–166. http://dx.doi.org/10.1038/nrm757

Peinado, H., E. Ballestar, M. Esteller, and A. Cano. 2004. Snail mediates E-cadherin repression by the recruitment of the Sin3A/histone deacetylase 1 (HDAC1)/HDAC2 complex. *Mol. Cell. Biol.* 24:306–319. http://dx.doi.org/10.1128/MCB.24.1.306-319.2004

Peña, P.V., F. Davrazou, X. Shi, K.L. Walter, V.V. Verkhusha, O. Gozani, R. Zhao, and T.G. Kutateladze. 2006. Molecular mechanism of histone H3K4me3 recognition by plant homeodomain of ING2. *Nature*. 442:100–103.

Pérez-Mancera, P.A., I. González-Herrero, M. Pérez-Caro, N. Gutiérrez-Cianca, T. Flores, A. Gutiérrez-Adán, B. Pintado, M. Sánchez-Martín, and I. Sánchez-García. 2005. SLUG in cancer development. *Oncogene*. 24:3073–3082. http://dx.doi.org/10.1038/sj.onc.1208505

Sauka-Spengler, T., and M. Bronner-Fraser. 2008. A gene regulatory network orchestrates neural crest formation. *Nat. Rev. Mol. Cell Biol.* 9:557–568. http://dx.doi.org/10.1038/nrm2428

Strobl-Mazzulla, P.H., and M.E. Bronner. 2012. Epithelial to mesenchymal transition: New and old insights from the classical neural crest model. *Semin. Cancer Biol.* http://dx.doi.org/10.1016/j.semcancer.2012.04.008.

Taneyhill, L.A., E.G. Coles, and M. Bronner-Fraser. 2007. Snail2 directly represses cadherin6B during epithelial-to-mesenchymal transitions of the neural crest. *Development*. 134:1481–1490. http://dx.doi.org/10.1242/dev.02834

Thiery, J.P., and J.P. Sleeman. 2006. Complex networks orchestrate epithelial-mesenchymal transitions. *Nat. Rev. Mol. Cell Biol.* 7:131–142. http://dx.doi.org/10.1038/nrm1835

Van de Putte, T., M. Maruhashi, A. Francis, L. Nelles, H. Kondoh, D. Huylebroeck, and Y. Higashi. 2003. Mice lacking ZFHX1B, the gene that codes for Smad-interacting protein-1, reveal a role for multiple neural crest cell defects in the etiology of Hirschsprung disease-mental retardation syndrome. *Am. J. Hum. Genet.* 72:465–470. http://dx.doi.org/10.1086/346092

Yochum, G.S., and D.E. Ayer. 2001. Pf1, a novel PHD zinc finger protein that links the TLE corepressor to the mSin3A-histone deacetylase complex. *Mol. Cell. Biol.* 21:4110–4118. http://dx.doi.org/10.1128/MCB.21.13.4110-4118.2001